Optimization of terminal airspace operation with environmental considerations

Yong Tian[a], Lili Wan[a], Ke Han[a,b,*], Bojia Ye[a]

[a] College of Civil Aviation, Nanjing University of Aeronautics and Astronautics, Nanjing 210016, China

[b] Department of Civil and Environmental Engineering, Imperial College London, United Kingdom

Abstract

The rapid growth in air traffic has resulted in increased emission and noise levels in terminal areas, which brings negative environmental impact to surrounding areas. This study aims to optimize terminal area operations by taking into account environmental constraints pertaining to emission and noise. A multi-objective terminal area resource allocation problem is formulated by employing the *arrival fix allocation* (AFA) problem, while minimizing aircraft holding time, emission, and noise. The NSGA-II algorithm is employed to find the optimal assignment of terminal fixes with given demand input and environmental considerations, by incorporating the *continuous descent approach* (CDA). A case study of the Shanghai terminal area yields the following results: (1) Compared with existing arrival fix locations and the first-come-first-serve (FCFS) strategy, the AFA reduces emissions by 19.6%, and the areas impacted by noise by 16.4%. AFA and CDA combined reduce the emissions by 28% and noise by 38.1%; (2) Flight delays caused by the imbalance of demand and supply can be reduced by 72% (AFA) and 81% (AFA and CDA) respectively, compared with the FCFS strategy. The study demonstrates the feasibility of the proposed optimization framework to reduce the environmental impact in terminal areas while improving the operational efficiency, as well as its potential to underpin sustainable air traffic management.

Key words: aviation emissions and noise, terminal airspace, approach, multi-objective optimization

Nomenclature

ATM:	*Air Traffic Management*
AFA:	*Arrival Fix Allocation*
ANP:	*Aircraft Noise and Performance*
CDA:	*Continuous Descent Approach*
ETA:	*Extended Terminal Area*
FAA:	*Federal Aviation Administration*
FBRP:	*Flow Based Route Planner*
FCFS:	*First Come First Served*
FF:	*Fuel Flow*
GA:	*Genetic Algorithm*
GB	*National Standard*
ICAO:	*International Civil Aviation Organization*
ISA:	*International Standard Atmosphere*
NPD:	*Noise Power Distance*

RNP: *Required Navigation Performance*
STAR: *Standard Instrument Arrival Route*
SID: *Standard Instrument Departure Route*
WECPNL: *Weight Equivalent Continuous Perceived Noise Level*

1. Introduction

With the significant growth of air transportation over the past decades, the associated environmental impacts have become a major concern to the public and authorities (Amato et al., 2010; Kurniawan and Khardi, 2011; Kinsey et al., 2011). When aircraft fly at low altitudes, e.g. in terminal airspace, they tend to negatively impact the environment and public health (Dolan et al, 2016). The terminal airspace provides capacity for arrival and departure routes that connect the runway(s) to the arrival and departure fixes. The mismatch of supply and continuously increasing demand has caused significant congestion at air traffic networks, especially at main bottlenecks such as the terminal airspace (Allroggen and Malina, 2014; Sidiropoulos et al., 2017). A lot of efforts have been dedicated by researchers and practitioners alike to the optimization of operations in the terminal area to alleviate congestion, improve operational efficiency, and reduce environmental impact of air traffic.

The environmental impact of aircraft activities in the terminal area is primarily attributed to the emission of greenhouse gases, pollutants and noises, which are highly related to public health given the relatively low altitude. The emission of pollutants is caused by incomplete combustion of fuel in the engine, which affects local air quality (Carslaw et al., 2008; Dodson et al., 2009; Barrett et al., 2013; Masiol et al., 2014, Planda et al., 2017), leading to adverse effect to the natural environment and public health (Kampa et al., 2008; Barrett et al., 2012, Barrett et al., 2015, Penn et al., 2017). Noise pollution, with the sound reaching 40dB and above, has been of widespread concern due to its impact on residential areas near the airport (Howarth and Griggs, 2013). High-volume noises can be irritating, affect daily life, and even have negative health effects (Clark and Stansfield, 2011; Fujiwara et al., 2017; Rodriguez-Diaz et al., 2017).

Aiming at the optimization of terminal airspace operation, existing studies tend to focus on the following aspects: runway allocation optimization, traffic flow sequencing, aircraft performance adjustment and terminal resource allocation. We provide a brief overview of these approaches below.

Regarding runway allocation optimization, Carr et al. consider the airlines' priorities to optimize arrival queues, which could reduce the economic impact of ATM restrictions and lead to increased airline economic efficiency by allowing airlines to have greater controls over their individual arrival banks of aircraft (Carr et al., 1999; 2000). Anagnostakis et al. (2001) establish a two-stage stochastic optimization model based on airport ground operation, with a focus on runway operations specifically for departure traffic. Sölveling et al. (2011) find that optimization-based scheduling with explicit environmental considerations tend to produce significant benefits for both airlines and society. Yin et al. (2014a, 2014b) put forward an optimization method for multi-runway spatio-temporal resource scheduling regarding the modes of dependent approaches and independent departures, which could significantly improve the service quality at busy airports.

On traffic flow sequencing, Bianco et al. (2006) propose a job-shop scheduling model with sequence-dependent setup times and release dates to coordinate both inbound and outbound traffic flows on all the predetermined routes of an airport terminal area and all aircraft operations at the runway complex. Balakrishnan et al. (2006) consider the problem of scheduling arrival aircrafts in a constrained position shifting environment and present a dynamic programming approach to maximize runway throughput. Based on the aircraft data total-energy model, Jin et al. (2013) establish an analytical relationship between speed, altitude, and fuel burn. The theoretical analysis suggests that speed profile has an impact on the fuel consumption as much as, if not more than, vertical profile in the terminal area. Kim et al. (2014) present an optimization model for simultaneously assigning aircraft to runways and scheduling the arrival and departure operations on those runways, to minimize the total emissions produced in the terminal area and on the airport surface.

Regarding aircraft performance adjustment, Mitchell et al. (2012) study the trade-off between CO2 and noise. The authors compared aircraft departure procedures subject to speed constraints with a free-flow scenario, and the results suggest that CO2 emissions could be reduced by 180 kg per flight if all the departure speed constraints were removed at a cost of increased noise exposure below 70dB. Silva et al. (2013) investigate the environmental impact of Required Navigation Performance (RNP) procedures, which seeks to improve fuel efficiency and reduce emissions by allowing noise to be concentrated in some areas near the airport. Marais et al. (2013) qualitatively describe measures to mitigate the environmental impact in each flight phase. Zhang et al. (2014) propose a noise assessment method based on track segment combined with civil aircraft motion model and performance model. Koudis et al. (2017) analyses the impact on fuel consumption and pollutant emissions by using reduced thrust takeoff. Ashok et al. (2017) calculate the minimum air quality and environmental impacts beyond fuel burn and CO2 minimization by optimizing gate holding and de-rated takeoffs.

Finally, regarding terminal resource allocation, Prete et al. (2004) develop a Flow-Based Route Planner (FBRP) system, which could handle a variety of constraints and efficiently route multiple flows of aircraft in dynamic weather scenarios. Given a flight route through the terminal area, Pfeil (2011), Pfeil and Balakrishnan (2012) apply machine learning techniques to optimize terminal area operations, by dynamically re-locating arrival and departure routes to maximize the expected capacity of the terminal area. In order to improve terminal operation efficiencies, Chen et al. (2013) present an algorithm for the integrated design of dynamic arrival and departure weather avoidance routing within extended terminal airspaces, Simaiakis et al. (2014) demonstrate the reduction of airport congestion through pushback rate control. Wan et al. (2016) establish an optimization model of arrival and departure resource allocation in terminal areas by considering factors such as airspace capacity and safety interval.

Attempts to mitigate environmental impacts of terminal airspace operation tend to focus on individual aircraft flight profiles (i.e. at a microscopic level). There is a lack of macroscopic modeling and optimization methods that aim to reduce the emission and noise in the entire terminal area. In this paper, we develop a multi-objective optimization framework based on *arrival fix allocation* (AFA) and *continuous descent approach* (CDA), aiming at reducing the congestion and environmental impacts of terminal operation under normal and adversarial weather conditions. To address the operation bottlenecks in the terminal area, we propose a concept to expand the terminal area and replace arrival fix holding in the terminal area with re-routing at the en-route descending phase. This leads to a multi-objective terminal area resource allocation problem to optimize AFA and reduce fuel consumption and noise in the terminal area through a coordinated use of CDA and resource distribution optimization model.

The rest of this paper is organized as follows. Section 2 elaborates the modeling details pertaining to emission, noise, and aircraft performance. In Section 3 we present the complete multi-objective optimization problem. A genetic algorithm is developed for the proposed optimization problem in Section 4. Section 5 details the Shanghai terminal area case study and analyzes the optimization results. Finally, Section 6 provides some concluding remarks.

2. Environmental impact of terminal area operation

Terminal area is a transitional region between en-route and airfield, which connects with air routes through arrival/departure fixes, and with airside through runways. The highly complex and interdependent operations make it a key bottleneck in air traffic flow management. At the same time, air pollution and noise produced by flights within the terminal area have a major impact on the surrounding environment. Modeling details pertaining to emission and noise are presented below.

2.1. Emission modeling

During the flight phase, the emissions mainly include NOx, CO, HC, CO_2, and SO_2. Among these pollutants, NOx, CO and HC are considered by control pollutant emissions of engine in ICAO annex 16 (volume II) (ICAO, 2014). Therefore, this paper considers the emissions of these three pollutants to describe the environmental impact of air traffic operation.

The aircraft pollutant emissions are typically related to the emission index (EI), fuel flow rate and discharge time. Let E_m denote the emissions of gas type m:

$$E_m = EI_m \cdot FF \cdot t \tag{1}$$

where EI_m represents emission index of gas m (g/kg), FF is fuel flow rate (kg/s), and t is the discharge time (s).

The operational characteristics of aircraft engine are related to the atmospheric conditions. The emission-related parameters are modified as:

$$FF = \frac{FF^R \cdot \delta}{\theta^{3.8} \cdot e^{0.2 \cdot M^2}} \tag{2}$$

$$EI_{NOx} = EI_{NOx}^R \cdot e^{CH} \cdot \left(\frac{\delta^{1.02}}{\theta^{3.3}} \right)^{0.5} \tag{3}$$

$$EI_{HC} = EI_{HC}^R \cdot \frac{\theta^{3.3}}{\delta^{1.02}} \tag{4}$$

$$EI_{CO} = EI_{CO}^R \cdot \frac{\theta^{3.3}}{\delta^{1.02}} \tag{5}$$

$$CH = -19.0 \times (HR - 0.00634) \tag{6}$$

$$HR = \frac{(0.62197058 \cdot R_H \cdot P_W)}{P - (R_H \cdot P_W)} \tag{7}$$

$$P_W = 611 \times 10^{\frac{7.5 \cdot T}{273.3+T}} \tag{8}$$

$$\theta = \frac{(273.15+T)}{288.15} \tag{9}$$

$$\delta = \frac{P}{101325} \tag{10}$$

where M is the Mach number, FF^R, EI^R_{NOx}, EI^R_{HC} and EI^R_{CO} respectively represent actual fuel flow rate (kg/s), and the emission indices of *NOx*, *HC* and *CO* in International Standard Atmosphere (g/kg). These parameters can be obtained via regression analysis based on data provided by ICAO engine emission database (EDB Version20), θ is the temperature ratio; δ is the pressure ratio; R_H is the relative humidity; HR is the humidity ratio; CH is the humidity coefficient; P_W is the saturated vapor pressure (Pascal); T is the atmospheric temperature (Celsius); and P is the pressure (Pascal).

Figure 1 shows the dual logarithm regression curve of CFM56-7B26's fuel flow rate and emission index (*NOx*, *HC* and *CO*), which are calculated by using the BFFM2 method (Baughcum et al., 1996).

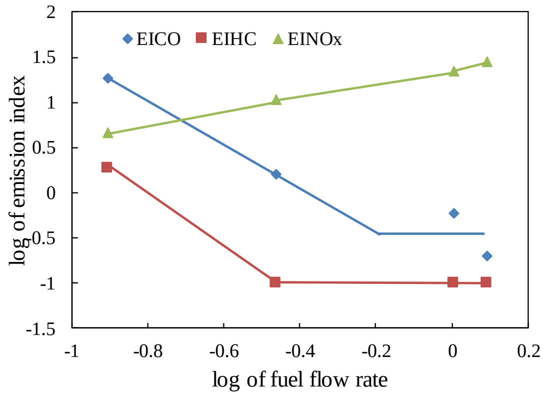

Figure 1. The log-log relationship between emission index and fuel flow rate (CFM56-7B26)

2.2. Noise modeling

In addition to fuel consumption and emissions, aircraft produce noises that affect residents near the airport when flying below 10000 feet. A diverse set of indicators has been employed around the globe to measure noise level near airports. Building on the ICAO guideline, China adapts the *weight equivalent continuous perceived noise level* (WECPNL), which is given by:

$$WECPNL = \overline{L_{EPN}} + 10 \cdot \lg(N_1 + 3 \cdot N_2 + 10N_3) - 39.4 \tag{11}$$

where N_1 is the number of aircraft in the daytime 07:00-19:00; N_2 is the number of aircraft in the evening time 19:00-23:00; N_3 is the number of aircraft in the nighttime 23:00-07:00. $\overline{L_{EPN}}$ denotes the average value of the effective perceived noise level, and can be calculated by the airport cumulative event noise. Note that the last term of (11) is adopted from National Standard of People's Republic of China (1988). We can calculate the single event noise by the split-run method, which is then summed up as the cumulative event noise:

$$\overline{L_{EPN}} = 10 \cdot \lg\left[\frac{1}{N \cdot T_0} \cdot \sum_i \sum_j \sum_k 10^{0.1 \cdot L_{EPNijk}(x,y)}\right] \tag{12}$$

where T_0 is the reference time, equal to 10 seconds, $L_{EPNijk}(x, y)$ represents single event noise level at point (x, y) when aircraft i is flying along the leg k of route j, which can be calculated by regression analysis and using the *NPD* data of *INM* or *ANP* (ICAO Doc9911).

2.3. Aircraft performance

The emissions and noise of aircraft are associated with the flight status and engine characteristics. The aircraft performance characteristics vary frequently with altitude and speed in terminal areas. The following dynamic model is used to populate a variety of realistic performance parameters.

The motion equation of the aircraft is established by the energy method:

$$(F_n - D) \cdot TAS = m \cdot g \cdot \frac{dh}{dt} + m \cdot TAS \cdot \frac{dTAS}{dt} \tag{13}$$

$$D = C_D \cdot \frac{1}{2} \rho \cdot TAS^2 \cdot S \tag{14}$$

Formula (13) represents the conversion between kinetic energy and potential energy of the aircraft under the action of the external force. Here in these equations, F_n is the engine thrust expressed as $\%T_R$, T_R denotes the rated thrust of the engine. Fuel flow (*FF*) of aircraft varies with the engine thrust. *D* is air resistance; m is mass; g is gravitational acceleration; *TAS* denotes true air speed; h is altitude; C_D is the resistance coefficient; ρ denotes air density; and *S* represents the wing area.

3. Optimization framework

In this paper, we consider the *extended terminal area* (ETA) approach as means to control and mitigate the emission and noise. We will achieve relevant objectives by optimizing the operation of terminal area based on the resource reallocation method. To facilitate problem specification, some assumptions/stipulations are given as follows.

(1) All aircrafts fly along the designated routes.

(2) Once the flights are assigned to the point of entry or start to take off, they cannot change STAR or SID.

(3) The arrival flights can be held only at the arrival fixes, while the departure flights can be held only on the ground.

(4) The arrival flights are allocated to the nearest runway at multi-runway airport.

(5) The operation mode and capacity of each runway are pre-determined under different weather conditions.

(6) No overtaking is allowed in the same STAR or SID.

(7) The spacing of arrival or departure are more than the ICAO-specified minimums.

3.1. Objective function

With environmental considerations, the overall aim of optimizing terminal area operation is to align the dynamic terminal airspace configuration, which may be subject to weather influence, with the runway system, in order to balance the dynamic demand and supply and reduce the impact of emission and noise. In this paper, we focus on three objectives: (i) emissions minimization, (ii) noise minimization, and (iii) balance of delays incurred at the arrival fixes. The third objective makes sure that the congestion is distributed evenly in the terminal area for equity considerations. That is, the delays at different arrival fixes are evenly distributed, leading to a spatial balance between airspace supply and demand.

3.1.1. Emission minimization

The total emissions can be expressed as the sum of normalized emissions of each pollutant, let EN denotes the sum of normalized emission:

$$\min EN = \min\left\{\sum_{m\in M}\left[Normal\left(E_m\right)\right]\right\} \tag{15}$$

where E_m is emissions of pollutant *m*; M is the set of pollutants. In this paper, $M = \{NOx, CO, HC\}$.

$$\begin{aligned} E_m = & \sum_{i\in A}\sum_{k\in F_A, w\in W}\lambda_{ik}^{w}\times\begin{pmatrix} t_i^h\cdot FF_i^h\cdot EI_i^{m,h} \\ +t_i^d\cdot FF_i^d\cdot EI_i^{m,d} \\ +t_i^a\cdot FF_i^a\cdot EI_i^{m,a}\end{pmatrix} \\ & +\sum_{i\in D}\left(S_i^D - E_i^D\right)\cdot FF_i^g\cdot EI_i^{m,g}\end{aligned} \tag{16}$$

$$\lambda_{ik}^{w} = \begin{cases} 1 & \text{if flight } i \text{ over the arrival fix } k \text{ within time window } w \\ 0 & \text{else}\end{cases} \tag{17}$$

where $EI_i^{m,h}, EI_i^{m,d}, EI_i^{m,a}$ and $EI_i^{m,g}$ denote the emission indices of pollutant m when flight i is held at arrival fix, descents, approaches and ground, respectively. A and D represents the arrival and departure flight set. W denotes the set of time window. F_A denotes the set of arrival fixes. t_i^h, t_i^d and t_i^a respectively denote the times of flight *i* being held at arrival fix, descents, and approaches. E_i^D and S_i^D denote the estimated and actual departure time. FF_i^h, FF_i^d, FF_i^a and FF_i^g respectively denote the fuel flow when the flight i is held at arrival fix, descents, approaches and ground.

Although the departure flights tend to produce more emissions than the arrival flights, it is difficult to decrease the departure flights' emissions in the climbing stage. Compared to the climbing stage, the departure flights' emissions on the ground is negligible and the optimization space is very limited in most airports. Therefore, the total amount of emissions excludes the emission from departure flights in the paper.

Aircraft emissions include several species such as CO_2, *NOx*, *CO*, *HC* and SO_2 (Dorbian et al., 2011; Penn et al., 2017). Among these *NOx*, *CO* and *HC* are selected in this paper since explicit guidelines are given by ICAO relating to the emissions of these species (ICAO, 2014). Regarding their relative importance in an optimization context, there exists few definite conclusions or guidelines in the literature as it largely depends on the specific situation and the decision makers' priorities. For this reason, and without loss of generality of the methodology, this paper makes a simplification by treating the three with equal weight/importance.[1] In addition, we do not include CO_2 in the objectives as it is highly correlated to the fuel burn, which has already

[1] In Torija et al. (2018), the relative weights of 0.4 (*HC*), 0.4 (*NOx*) and 0.2 (*CO*) were adapted, and we have performed the optimization proposed in this paper for these weights. The results are presented in the Appendix.

been considered by the optimization. Nevertheless, to demonstrate that the proposed method works equally for other types of pollutants such as SOx, CO_2, and PM, we will show in Figure 16 that the optimized strategies could significantly reduce those emissions as well, although they are not explicitly optimized in our paper.

Moreover, for minimizing emissions it is sometimes considered sufficient to minimize fuel burn (Solveling et al., 2011). However, while the emission of CO_2 may be aligned with fuel consumption, it is unclear how the emissions of other pollutants (NOx, HC, CO) are related to fuel burn. To understand the levels of alignment between the objectives of fuel burn and emissions, we present some additional experiments in the Appendix.

3.1.2. Noise minimization

There exist a number of different criterion for minimizing noise pollution in the literature (Basner et al., 2014; Wolfe et al., 2016). This paper aims to minimize the areas around the terminal airspace with noise levels above 70dB, following the environmental standard of aircraft noise near airports (GB9660-88). Such a choice is informed by the particular situation in China, which, as a developing country, has most of its commercial airports located in less populated areas, typically on the outskirts of cities. This will inform policy and decision making regarding future land use near airports, given the expected population increase in these areas due to rapid urbanization and convenient transportation.

According to the environmental standard of aircraft noise near airports (GB9660-88), the level of sound in residential areas should be below 70dB. Given such a constraint, we aim to reduce the impact of noise in terminal areas by minimizing the spatial extent of sound levels above 70dB:

$$\min\left\{sqare\left(L_{WECPN}\left(x,y\right)>70\right)\right\} \tag{18}$$

where $square(L_{WECPN}(x,y) > 70)$ denotes the area of regions in the 2-dimensional plane where the sound level is above 70dB.

Different choices of approach profiles lead to varying aircraft performance parameters such as altitude, speed, and heading, and will result in the variation of approach time and fuel flow, hence the level of fuel consumption and emissions. When approaching along the traditional STAR, the aircraft fly at low altitude for much of the approach time and the noise has more influence on the residents. However, the CDA mode can extend the time when aircraft fly at high altitude and reduce the effect of noise pollution.

Taking the STAR (SASAN-11A) of Shanghai terminal area as an example, we calculate the WECPNL noise level when a B738 aircraft approaches along the traditional STAR as well as under the CDA mode, the corresponding noise contours are shown and compared in Figure 2.

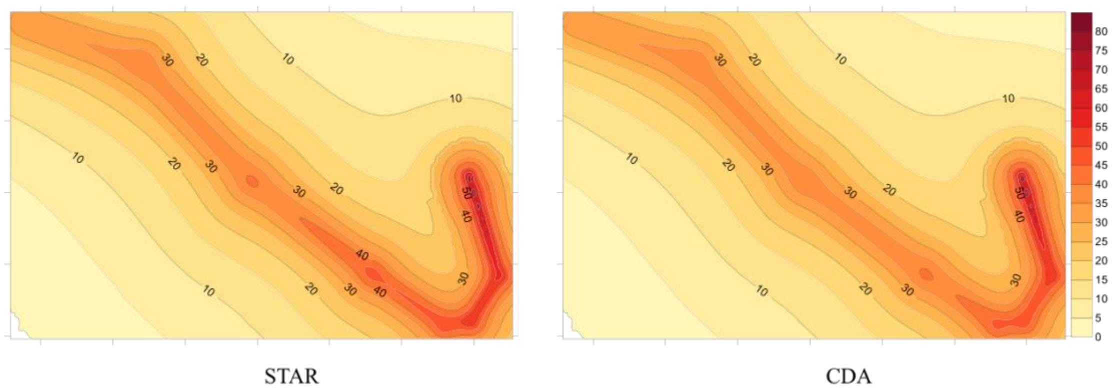

Figure 2. The noise contours under STAR (left) and CDA (right) approach mode(dB)

The high-noise levels are mainly concentrated in the approach path on final and final turn, and the noise of the rest segment is relatively small. It can be seen from Figure 2 that the overall noise level has declined under the CDA mode, and that the range of WECPNL noise contour between 40-45 dB is significantly narrowed.

3.1.3. Balance of delays at arrival fixes

Unbalanced traffic flow or capacity of arrival fixes will result in the delay concentrating on some arrival fix. Such situations can be avoided in our formulation by re-assigning traffic to alternative fixes. Therefore, the balance of holding times at all the fixes, as expressed below, leads to a balanced distribution of airspace supply and delay. In order to ensure equitable distribution of arrival resources, we define the following objective to be minimized:

$$\min \sum_{k \in F_A} \left| T_k^h - T^h \right| \tag{19}$$

where $T_k^h = \sum_{i \in A, w \in W} \lambda_{ik}^w \cdot t_i^h$ is the holding time of arrival fix k. F_A denotes the set of arrival fixes. $T^h = \left(\sum_{k \in F_A} T_k^h\right) / |F_A|$ is the average holding time of all arrival fixes.

3.2. Constraints of the optimization problem

(1) Unique fix condition

When a flight is approaching, it can be assigned to only one arrival fix, this can be expressed by:

$$\sum_{k \in F_A} \sum_{w \in W} \lambda_{ik}^w = 1 \tag{20}$$

(2) Capacity constraints

The total of flights via the arrival fix cannot exceed the capacity of this fix within one time window. The total of flights that take off and land on the runway cannot exceed the capacity of runway within one time window.

$$\sum_{i \in A} \lambda_{ik}^w \le C_k^w \quad k \in F_A \tag{21}$$

$$\sum_{i \in A \cup D} \xi_{ir}^w \le C_r^w \quad r \in R \tag{22}$$

where C_k^w is capacity of the arrival fix k in time window w, C_r^w is capacity of the runway r in time window w, and when flight i uses runway r in time window w, ξ_{ir}^w is equal to 1, or equal 0 otherwise.

(3) Maximum air holding time

The air holding time of each arrival aircraft cannot exceed the maximum air holding time at arrival fix.

$$t_i^h \leq T_{\max}^h \quad i \in A \tag{23}$$

where T_{max}^h is the maximum air holding time. To ensure flight safety, China Civil Aviation Regulations (CCAR 2016) stipulate that aircraft should carry enough fuel for being held by up to 45min (domestic) or 30min (international) over the destination airport. Therefore, T_{max}^h is set to be 45min or 30min, depending on the type of flights.

4. Design of optimization algorithm

Since the terminal area contains two or more airports, a larger number of air traffic flow and routes make a great calculating workload when we search the optimal solution. Therefore, non-dominated sorting genetic algorithm with elitist strategy (NSGA-II) (Deb et al., 2002; Srinivas and Deb, 1994) is selected to solve the problem in this paper. The NSGA-II is one of the most popular MOO algorithms, the high performance of NSGA-II for finding Pareto solutions is dependent on its evolution mechanisms, mainly including the fast non-dominated sorting, crowing distance, and non-dominated ranking-based elite preservation strategy. NSGA-II algorithm enjoys a few advantages over other multi-objective algorithms. Existing algorithms tend to apply a single fitness function or convert multiple objectives to a single one (through scalarization), which may lose some important features. On the other hand, NSGA-II handles the multiple objectives by finding Pareto efficient solutions. In addition, it has the advantages of good convergence and computational efficiency, which meets the requirement of real-time operation. For the problem of terminal area operations optimization, the steps of the NSGA-II algorithm are as follows.

Step 1: Population Initialization

For this problem, each solution is defined by an individual p containing three sub-chromosomes in real mode with $3n$ genes. Each sub-chromosome contains n genes representing part of the arrival time-space information. As shown in Figure 3, ra_i is the descent route gene of flight f_i which reveals the proposed descent route from the edge point of ETA to the arrival fix, ap_i is the arrival fix gene of flight f_i which represents the extra holding time at the arrival fix, and ar_i is the STAR gene of flight f_i which shows the usage of traditional or CDA arrival routes. Let RA_{max} be the number of alternative descent routes, AP_{max} be the maximum en-route holding time (measured in minutes), AR_{max} be the number of alternative STAR routes. Then, the genes ra_i, ap_i and ar_i of each flight f_i are generated in their corresponding boundary using a uniform distributed random function. For example, a gene $[rai\ api\ ari]T = [2\ 15\ 2]T$ means that the flight f_i chooses the second descent route to the arrival fix point, and after 15 minutes holding at that fix point, it will select the second STAR route (CDA) to descend to the runway.

f_1		…………		f_i		…………		f_n
ra_1				ra_i				ra_n
ap_1				ap_i				ap_n
ar_1				ar_i				ar_n

Figure 3. The schematic diagram of chromosome coding of GA

The original time when the flight enters into ETA can be calculated based on the scheduled route and arrival time. According to the information of ETA's entry point and distributive runway, RA_{max} and AR_{max} can be initialized for each flight. And the value of AP_{max} is determined by the users. Then, the population with NP individuals can be initialized based on the proposed chromosome. Also, to ensure that the initial population's otherness and increase the possibility of obtaining the global optimal solution, the number of chromosome whose hamming distance in population is greater than a pre-set value must exceed a certain ratio.

Step 2: Non-Dominated sort

Before selection calculation, population should be layered and sorted to form multiple Pareto fronts with different ranks based on the domination level of each member determined by its own value of objective functions. This procedure is repeated until all solutions are set into fronts. Consider the information of aircraft types, initial speeds, and initial attitudes of all the flights, the total emission, noise and delays can be calculated based on the models introduced in section 2. The fitness of three objective of terminal area operations optimization model is designed as:

$$Fit_1 = \left(\sum_{m \in M} \left[Normal\left(E_m\right) \right] \right)^{-1} \tag{24}$$

$$Fit_2 = sqare\left(AS\right) - sqare\left(L_{WECPN}\left(x, y\right) > 70\right) \tag{25}$$

$$Fit_3 = \left(\sum_{i \in A} \left| t_i^h - \overline{t_i^h} \right| \right)^{-1} \tag{26}$$

where $sqare\left(AS\right)$ is the area of the noise scope of evaluation.

Step 3: Crowding Distance

Once the non-dominated sort is complete the crowding distance is assigned. Since the individuals are selected based on rank and crowding distance all the individuals in the population are assigned a crowding distance value. Crowding distance is assigned front wise and comparing the crowding distance between two individuals in different front is meaningless. The crowding distance of jth individual (L[j]) is defined as following:

$$L[j] = \sum_{k=1}^{3} (L[j+1] \cdot Fit_k - L[j-1] Fit_k) / (Fit_k^{\max} - Fit_k^{\min}) \tag{27}$$

Step 4: Selection and genetic operation

Once the individuals are sorted based on non-domination and with crowding distance assigned, the selection is carried out using a crowded comparison. The comparison is carried out based on non-domination rank and crowding distance.

In this research, parent population is generated by binary tournament method, and progeny population is obtained by crossover and mutation. Chromosomes of progeny population will generate a new arrival time according to the aircraft's entering time, the route information of descent and approach. Mix arrival and departure aircraft to a flight queue and sort them with those runway time, then reject the chromosome, which are not meeting the constraint conditions and update the arrival time and arrival fix time of the remaining chromosome. Combine progeny population and parent population, and calculate fitness value of each chromosome. Use elite strategy to keep the better chromosome to generate a new parent population.

Step 5: Recombination and Selection

The offspring population is combined with the current generation population and selection is performed to set the individuals of the next generation. Since all the previous and current best individuals are added in the population, elitism is ensured. Population is now sorted based on non-domination. The new generation is filled by each front subsequently until the population size exceeds the current population size. Then, some of individuals in this front are selected based on their crowding distance in the descending order until the population size is *N*. And hence the process repeats to generate the subsequent generations.

5. Numerical case study

5.1. Description of the test site

The case study focuses on the Shanghai terminal area, which serves ZSPD (Pudong International Airport) and ZSSS (Hongqiao International Airport). Both of the airports have multiple runways, with high volume of traffic flow and limited airspace resources. In fact, the Shanghai terminal area has been known as one of the busiest multi-airport terminal areas in China. We consider three strategies for terminal area operation: FCFS (first come first serve), AFA (arrival fix allocation) [16] and AFACDA (arrival fix allocation and continuous descent approach).

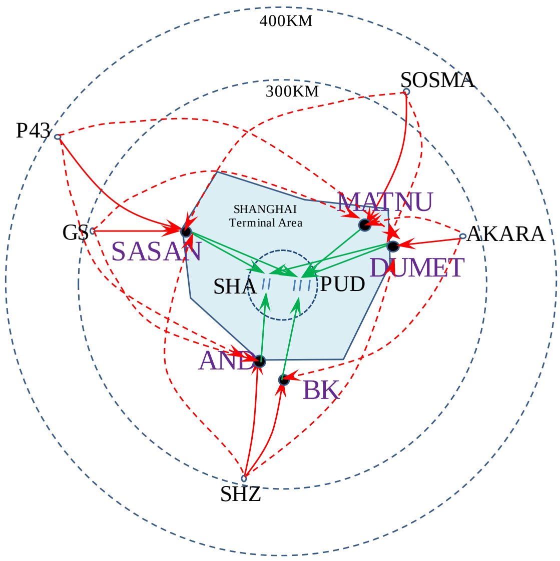

Figure 4. Sketch of Shanghai terminal area with 5 approach fixes shown.

The size of ETA is set as 400km, five en route waypoints GS, SHZ, AKARA, SOSMA and P43 are chosen as the edge points of ETA, five fixes that are used for approach are AND, BK, DUMET, MATNU and SASAN, as shown in Figure4. In practical, each waypoint can link only one or two arrival fix points. In the experiment, assume that two more adjacent arrival points are connectable for each en route waypoint. The connectivity and the length of each links are shown in Table 1.

Table 1. The connectivity and the length of descent routes (km)

Waypoint \ Arrival Fix	AND	BK	DUMET	MATNU	SASAN
GS	301	-	-	345	124
SHZ	96	61	307	-	428
AKARA	-	321.8	71.4	112	-
SOSMA	-	-	432	247	444
P43	462	-	-	460	196

Usually, the handover separation of terminal area is 20 kilometers in the same direction and altitude. In the event of severe weather, the handover separation needs to be increased, resulting in the reduction of the arrival fix capacity. It is envisaged that severe weather could occur in the Shanghai Terminal Area, and the capacity changes of arrival fixes under severe weather are shown in Table 2. The capacity of SASAN is reduced from 25 to 15 sorties/hour. So we plan to optimize the aircraft operations in terminal airspace, and assume that both STAR and CDA can be used at each arrival point.

Table 2. The capacity change of arrival fixes under severe weather.

Arrival fix	Normal capacity (sorties /hour)	Reduced capacity (sorties /hour)
AND	25	25
BK	25	25
DUMET	25	25
MATNU	25	25
SASAN	25	15

We simulate the air traffic flow of ZSPD and ZSSS during the period 11:00-17:59 on one typical day, and apply different strategies to the terminal area operation and conduct a comparative study on their results. During the simulation period, the total number of flights in the Shanghai terminal area is 735, of which 426 are from/to ZSPD and 309 flights are from/to ZSSS. Runways 34 and 35L are used for landing and runways 34, 35R are used for take-off in ZSPD; Runway 36R is used for landing and runway 36L is used for take-off in ZSSS.

There are 16 different aircraft types among these flights, and six aircraft types are more than 5% which are A319 (6%), A320 (35%), A321 (9%), A330 (10%), B737 (18%), B747 (7%) and B777 (7%). The simulation program is written in the MATLAB, all the aircraft performance parameters used in this research, such as the thrust coefficients, engine types, aerodynamics parameters, fuel flow parameters, come from the *User Manual for the Base of Aircraft Data* (BADA) published by EUROCONTROL. Table 3 shows some of the assumption data and operational environmental parameters for different aircraft, including the aircraft mass (m), the initial true airspeed (TAS) at each ETA waypoint and arrival fix, aircraft initial altitude at ETA waypoint and arrival fix.

Table 3. Aircraft performance parameters

Aircraft type	Mass (kg)	velocity at ETA waypoint	velocity at Arrival fix (kn)	Altitude (m) at ETA waypoint	Altitude (m) at Arrival fix
A319	60,000	.79/300	300	7,800	6,000
A320	64,000	.79/300	310	7,800	6,000
A321	72,000	.78/300	300	7,800	6,000
A330	174,000	.82/300	300	7,800	6,000
B737	65,300	.78/290	290	7,800	6,000
B747	285,700	.86/310	310	7,800	6,000
B777	208,700	.84/300	300	7,800	6,000

In the experiment, NSGA-II algorithm control parameters are set as follows: population size is 300, the termination generation of GA is 200, crossover probability is 0.8, and mutation probability is 0.01, the elite strategy keeps 8 best chromosomes for each generation. The linear recombination cross and stochastic factor mutation rule are used in the implementation of genetic manipulation.

The program is written in the C++ language, the computational times were 3 minutes for each replication by IMB250 with 6GHz AMD A8 CPU and 4G RAM.

5.2. Analysis of results

Figure 5 shows the distribution of the individuals in the population corresponding to the termination algebra. Under the premise of keeping population diversity, we can obtain the Pareto optimal solution by using Multi-objective genetic algorithm. In Figure 5, the blue spheres indicate the non-dominated solutions on the Pareto front. Figure 6 shows some non-dominated solutions set corresponding to the Pareto front of the termination algebra.

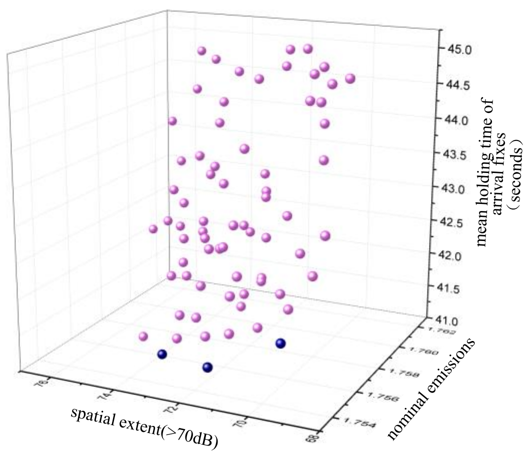

Figure 5. Population distribution of the termination algebra of genetic algorithm (AFACDA)

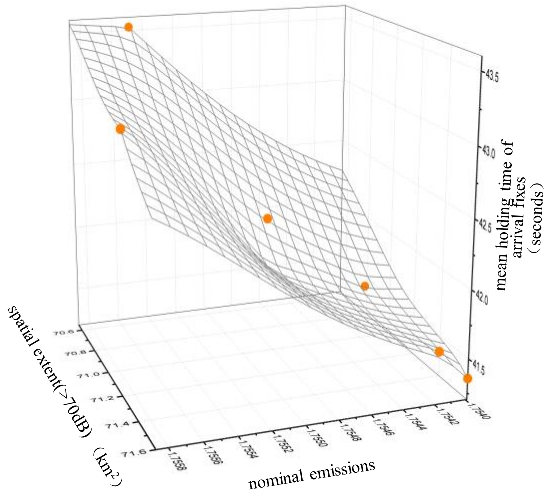

Figure 6. Pareto front with AFACDA strategy

The normalized emissions reduce from 1.879 to 1.786 within 50 generations by optimizing calculation with AFACDA strategy. From 50 to 100 generations, the decline of normalized emissions becomes slower and the value reduces to 1.782, and the value will tend to be stable with very small fluctuation after 100 generations, as shown in Figure 7.

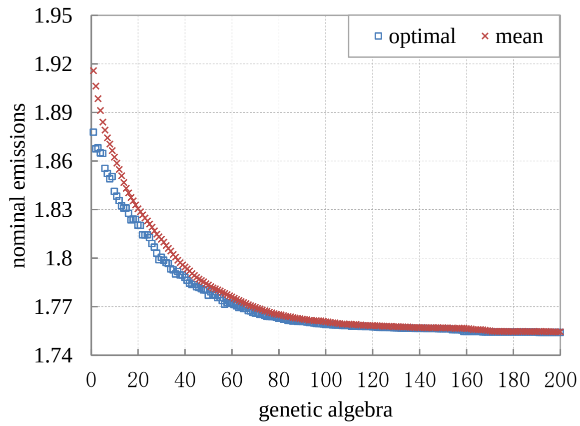

Figure 7. The variation of the normalized emissions with the genetic algebra under the AFACDA strategy

The Pareto solutions shown in Figure 6 are further elaborated in Table 4. Overall, it can be seen that the holding times decrease while the emissions decrease, but the noise level may increase at the same time. This suggests that the three objectives considered are not aligned with each other, and apparent trade-offs exist (e.g. between holding time and noise). In addition, the efficiency of such trade-offs vary; for example, a relatively small change in the emissions (between 1.7540 and 1.7559) leads to a more significant change in the holding times (between 16424 and 17126). This calls for additional information regarding the decision maker's priorities towards these different objectives. Moreover, as seen in Figure 6, the emission-noise relationship is not entirely monotone, which reveals further complexities of the problem under investigation, and necessitates quantitative and optimization based approaches such as the one proposed in this paper.

Table 4. Alternative Non-dominated designs for AFACDA strategy

AFACDA alternative designs	Nominal emissions	Spatial extent (>70dB)(km^2)	The average holding time (s)
1	1.7540	71.6000	41.4
2	1.7541	71.5633	41.5
3	1.7542	71.0876	41.7
4	1.7550	71.1730	42.4
5	1.7555	70.5464	43.5
6	1.7559	71.2523	43.1

Compared with FCFS, the emissions of *NOx*, *HC* and *CO* can be reduced by using the AFACDA strategy. Among all the flight phases, holding at arrival fixes experience the most significant reduction of emissions, as shown in Figure 8, Figure 9 and Figure 10. The *NOx* emission index is greater than *HC* and *CO* when aircrafts fly in terminal area, so the decrement of *NOx* emissions is the most obvious. AFACDA strategy achieves the purpose of optimizing allocation of air traffic flow at arrival fixes by changing the descent route. The strategy may lead to the increment of the descending time and various emissions. As shown in Figure 8, these parameters increase by about 1%.

Compared with AFA, the emissions of descent, holding on arrival fixes and ground change little by using the AFACDA strategy. However, the emissions of approaching further reduce because of choosing CDA. The reduction is up to 20%, as shown in Figure 8, Figure 9 and Figure 10. Therefore, the AFACDA strategy is efficient to reduce emissions when handling the problem of capacity decrease or unbalance traffic flow.

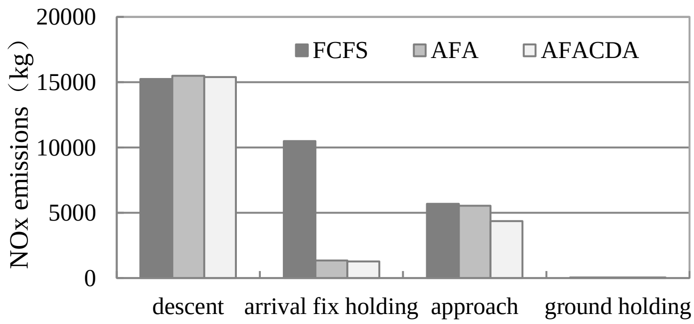

Figure 8. Comparison of *NOx* emissions with different strategies

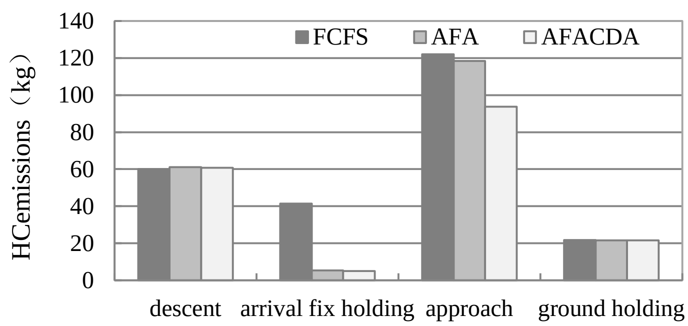

Figure 9. Comparison of *HC* emissions with different strategies

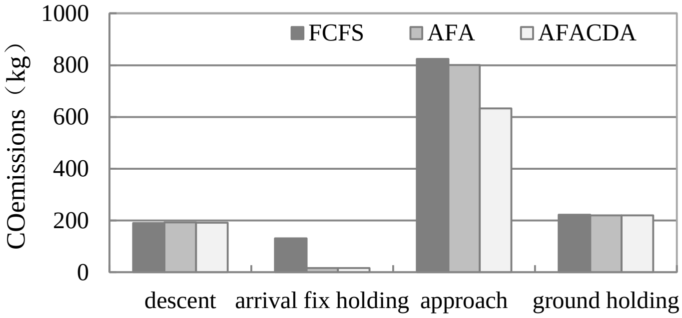

Figure 10. Comparison of *CO* emissions with different strategies

Based on the combination of the CDA mode and optimizing the allocation of arrival fixes (AFA), the resulting noise contour map of the terminal area is shown in Figure 11, where the blue points are the arrival fixes. A similar contour map is shown for the AFA strategy (without CDA) in Figure 12. For ease of comparison between the two cases, we plot the difference (AFA-AFACDA) of the noise levels in Figure 13.

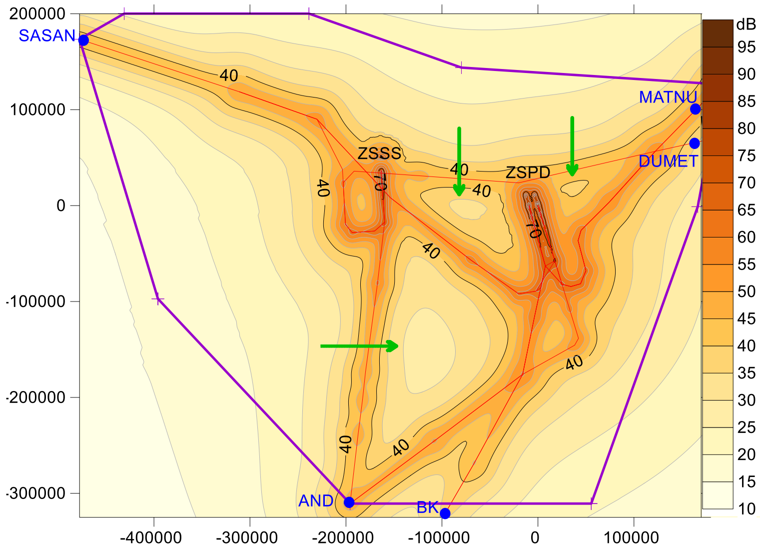

Figure 11. The noise contour of Shanghai terminal area (AFACDA strategy)

It can be seen from Figure 13 that, by employing the CDA within the AFA framework brings additional savings, and the areas affected are mostly concentrated along the flight routes in the terminal area near the final approaches and the final turns.

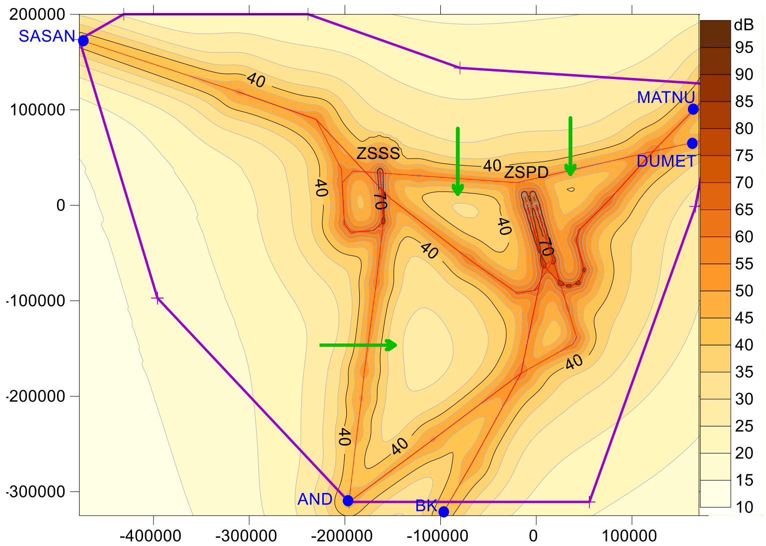

Figure 12. The noise contour of Shanghai terminal area (AFA strategy)

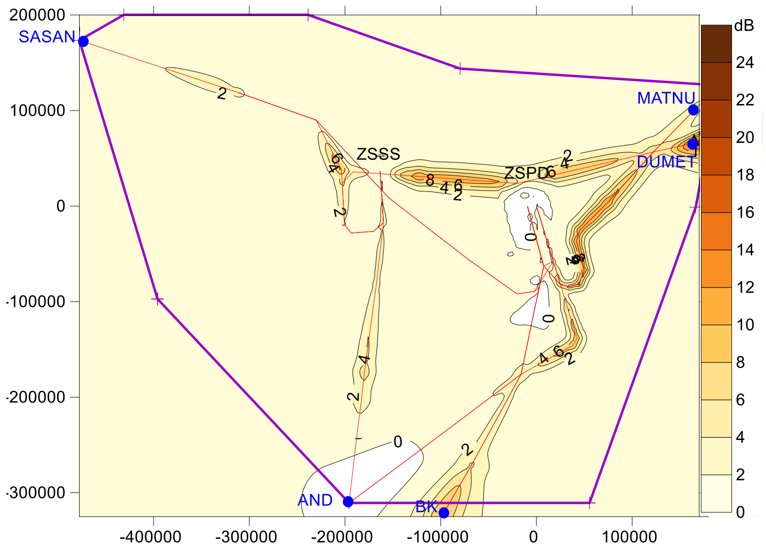

Figure 13. Difference of noise levels between AFA and AFACDA.

The conventional mode, which embraces the first-come-first-serve (FCFS) principle, is implemented, whose resulting noise contour map is shown in Figure 14. Similar to before, we plot the difference between the FCFS and AFACDA approaches, in Figure 15. Compared to Figure 13 (AFA-AFACDA), Figure 15 suggests that the combination of AFA and CDA produces the least noise in the terminal area, although applying each in isolation does also result in gain in noise efficiency.

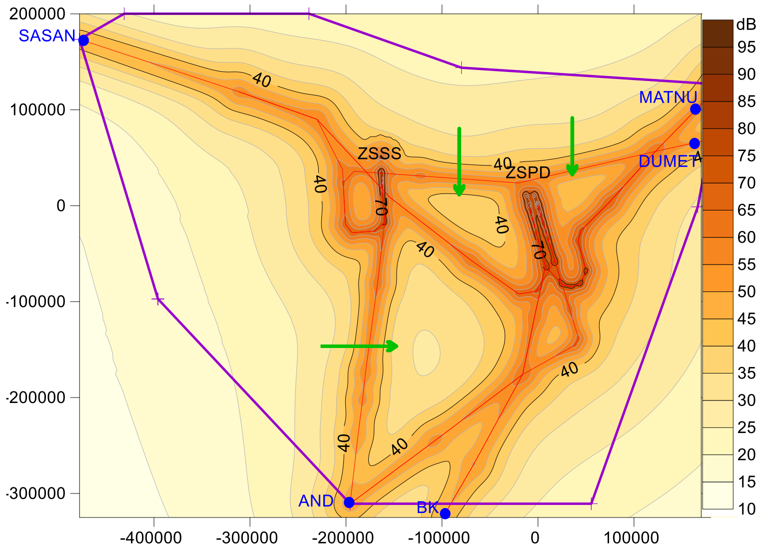

Figure 14. The noise contour of Shanghai terminal area (FCFS strategy)

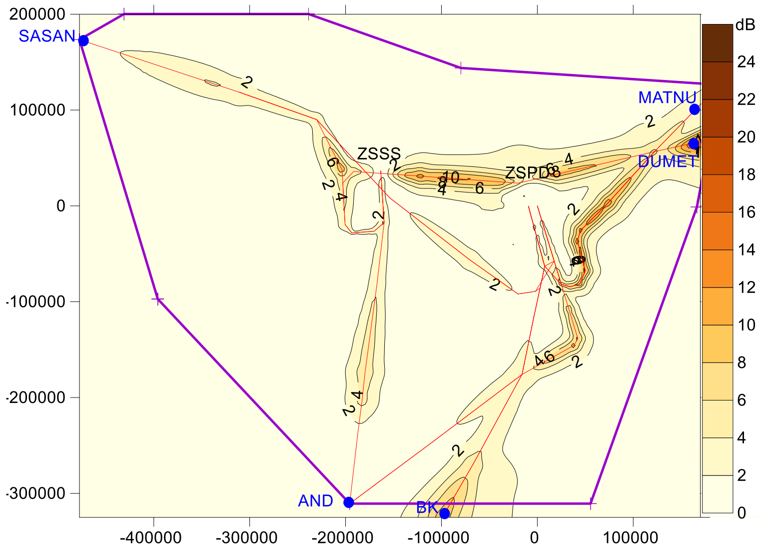

Figure 15. Difference of noise levels between FCFS and AFACDA.

According to GB9660-88, if the noise level is between 70dB and 75dB, the land can be planned for living quarters in addition to special housing, residential and cultural areas. By using CDA mode, the influenced areas of noise level above 75 dB are mainly distributed near runway and final approach, the spatial extent are shown in Table 5. Comparing the AFA strategy with AFACDA, the influenced areas (with dB above 70) within the Shanghai terminal area is narrowed by 26%.

Table 5. Comparison of noise range in different approach modes

Noise level (dB)	Spatial extent (km^2)					
	Pudong airport			Hongqiao airport		
	FCFS	AFA	AFACDA	FCFS	AFA	AFACDA

≥75	30.8	23.9	22.6	6.9	6.2	4.5
70 ~75	59.8	53.7	36.8	18.2	12.9	7.7

In this paper, we assume that the capacity of SASAN reduce in case of severe weather. When using FCFS strategy, the total holding time in SASAN reaches 132,313.7 seconds, accounting for 84% total holding time of all arrival fixes, and the average holding time is 842.4 seconds per flight. The delay is severe and highly concentrated. In addition, 89.5% of arrival flights in SASAN are delayed due to insufficient capacity, the maximum holding time is up to 2351.4 seconds, while 92% of flights in the other four arrival fixes only need to hold 240 seconds or less. Using FCFS strategy, we will find the holding time of arrival fixes is unbalance, total delay is large and the airspace resources are not used to the full.

Once choose AFA and AFACDA strategy to reallocate the arrival fixes, the average holding time in SASAN reduce to 55.7 seconds per flight and 50 seconds per flight respectively, and the average holding time of all flights reduce to 45.1 seconds per flight and 43.3 seconds per flight respectively. The delay of arrival fixes is relatively balance and significantly alleviate, as shown in Figure 16. The AFACDA strategy proposed in this paper can achieve to balance and relieve arrival fixes delay by rerouting in the descent phase of the en-route and reassign the traffic flow of arrival fixes.

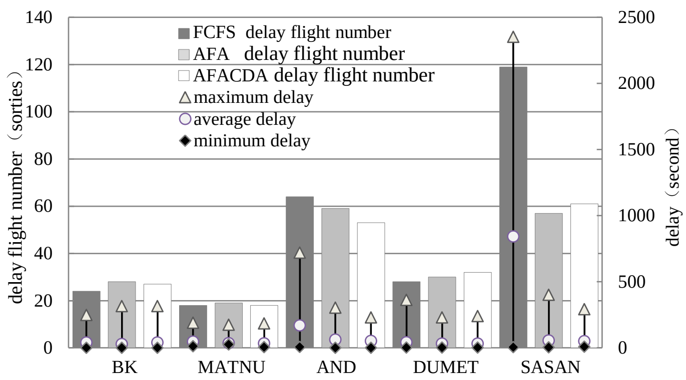

Figure 16. Comparison of holding time of arrival fixes with different strategies

The AFACDA strategy can not only reduce emission and noise levels, but also improve the efficiency of terminal area operation, as shown in Figure 17. Compared with FCFS, AFACDA increases the percentage of flights with delays below 5 minutes from 80.6% (FCFS) to 93.6% (AFACDA), and reduces the percentage of flights with delays above 15 minutes from 8.9% to 0.8%. The average delay among all the flights decreases from 3.9 min to 1.6 min. Therefore, the operating efficiency of terminal area is significantly improved alongside environmental objectives.

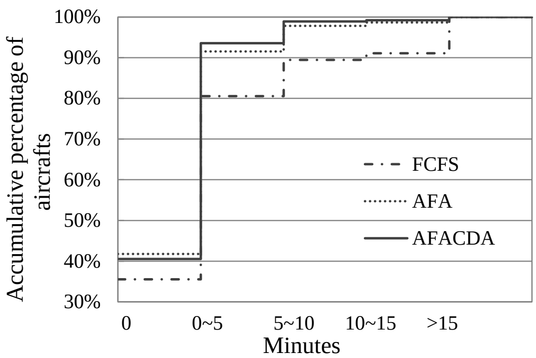

Figure 17. Comparison of delay distribution with different strategies

Although not explicitly optimized in our method, other types of pollutants: SOx, CO_2 and PM are also significantly improved after using AFA and AFACDA strategies, as shown in Figure 16. (The emission indices of SOx and CO_2 are 1.1712g/kg and 3.155g/kg respectively, The emission index of PM can calculate by the data of ICAO databank [AEDT 2c 2016]).

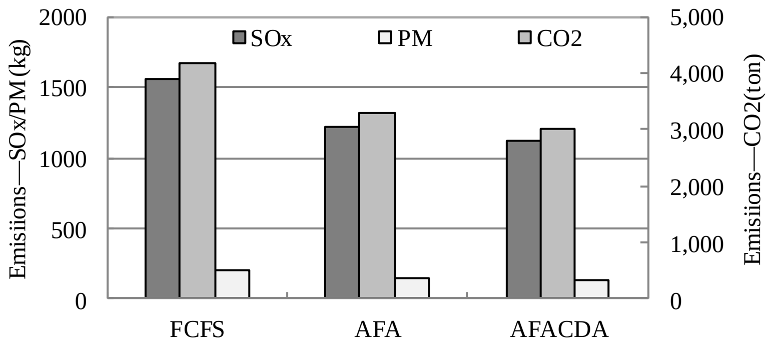

Figure 16. Other emissions with different strategies

6. Conclusion

This paper proposes an optimization framework for terminal operations with environmental considerations, by incorporating a multi-objective terminal area resource allocation problem. The objectives include aircraft emissions, noise level, and holding delays (for arrivals). An arrival fix allocation (AFA) problem is combined with a continuous descent approach (CDA) and optimized using the NSGA-II algorithm with given air traffic demand. A case study of the Shanghai terminal area during peak operational period (11:00-17:59) on a typical day reveals that

(1) Compared with existing arrival fix locations and the first-come-first-serve (FCFS) strategy, the AFA reduces the emissions by 19.6%, and the areas impacted by noise by 16.4%. AFA and CDA combined reduce the emissions by 28% and noise by 38.1%.
(2) The flight delays caused by the imbalance of demand and supply can be reduced by 72% (AFA) and 81% (AFACDA) respectively, compared with the FCFS strategy.

On the environmental aspects, this paper mainly focuses on the emissions of air pollutants and noises. Additional modeling efforts are needed to assess the public exposure to air pollutants and noises. This would entail much richer datasets concerning not only the population distribution and activity patterns, but also the meteorological and chemical environments. Pollutant dispersion models for the study area also need to be developed and incorporated within our optimization framework. These are beyond the scope of this single paper, which aims primarily at developing a holistic framework for the resource allocation problem in terminal airspace with environmental objectives. Moreover, the inclusion of public exposure as objectives, provided that additional data and models are available, would likely result in quantitatively different decision variables. This, however, does not undermine the usefulness of this paper as a reference for decision making.

The proposed framework may be applied to strategic or pre-tactical levels, with given information of flight schedules. Its applicability and effectiveness in a real-time operational environment will be assessed with stochastic or robust optimization given real-time updates of flight information (Sidiropoulos et al. 2017). Nevertheless, changing the routing structures within the terminal areas need to undergo comprehensive assessment involving multiple stakeholders, and the resulting impact on the ATC workload could be a potential issue. In addition, the uncertainties in the air traffic demand need to be addressed within this framework with a stochastic or robust optimization approach if the framework is to be adapted to an operational or near real-time level.

Appendix

Sölveling et al. (2011) determine that solving problems that minimize fuel burn are typically sufficient for minimizing emissions of CO_2. However, it is unclear how the emissions of other pollutants such as *NOx*, *HC*, and *CO* are related to fuel burn. To investigate this issue, and to justify the explicit minimization of emissions conducted in our paper, we perform the optimization by (a) minimizing fuel burn only, and (b) minimizing different species of emissions. Table6 shows the performances of these solutions. It can be seen that minimizing fuel consumption does not necessarily minimize emissions of different species, and it is therefore necessary to explicitly model and optimize the latter.

Table 6. Comparison of fuel consumptions in scenarios (a) and (b)

	NOx(g)	*HC*(g)	*CO*(g)	Nominal emission	Fuel(kg)
(a) min(fuel)	20738732	181833	1057284	1.7372	912251
	2.67% Lower than (b)	3.46% Higher than (b)	4.05% Higher than (b)	2.97% higher than (b)	-
(b) min(emission)	21307618	175747	1016202	1.6871	928205
	-	-	-	-	1.75% higher than (a)

Next, we examine the effect of changed weights for *HC*, *NOx* and *CO* in the objective function. Unlike the equal weights assumed in Section 5, Torija and Self (2018) develop alternative scaling factors to take into account the trade-offs between different species and noise. Following their paper, we conduct a new experiment with the weights of 0.4 (*HC*), 0.4 (*NOx*) and 0.2 (*CO*) in the objective function. The resulting Pareto front is shown in Figure 18.

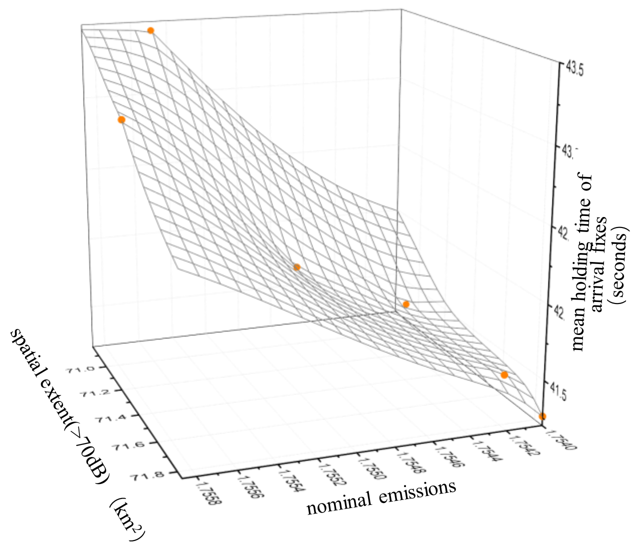

Figure 18. Pareto front with the new weights of 0.4 (*HC*), 0.4 (*NOx*) and 0.2 (*CO*).

The emissions corresponding to different operational strategies are shown in Figure 19-Figure 21.

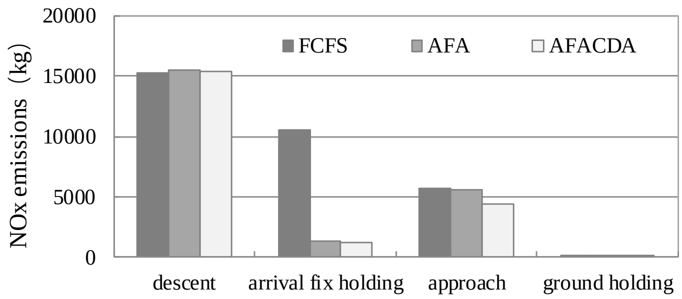

Figure 19. *NOx* emissions corresponding to different approach modes

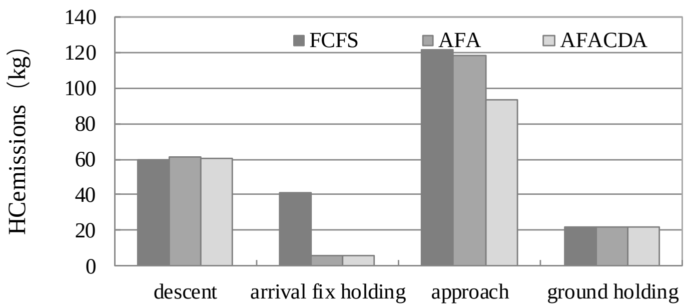

Figure 20. *HC* emissions corresponding to different approach modes

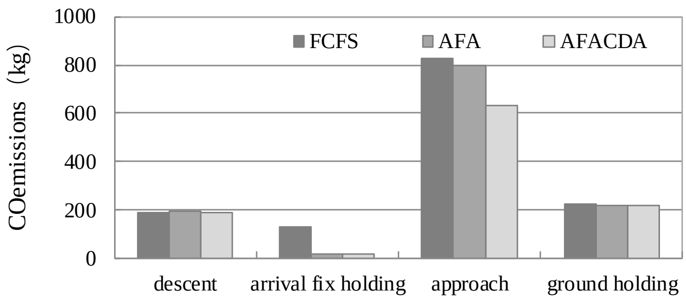

Figure 21. *CO* emissions corresponding to different approach modes

The areas affected by noise pollution under different strategies are shown in Table7.

Table 7. Noise range corresponding to different approach modes

Noise level (dB)	Spatial extent (km²)					
	Pudong airport			Hongqiao airport		
	FCFS	AFA	AFACDA	FCFS	AFA	AFACDA
⩾75	30.8	24.0	22.7	6.9	6.3	4.7
70 ~75	59.8	54.2	37.1	18.2	13.1	7.8

Compared to the 1:1:1 weight, the results have discernible changes. In particular, the emission of *NOx* has reduced while the emissions of both *HC* and *CO* have increased. The decrease of *NOx* is due to its increased relative weight in the objective function, which means that the aircraft needs to enter the descent phase sooner to reduce thrust and the emission factor of *NOx*. Meanwhile, the emission factors of *HC* and *CO* will increase, leading to increased *HC* and *CO* emissions. The earlier descent means that the noise range will increase.

Acknowledgment

This research was supported by the National Natural Science Foundation of China (Grant Nos. 61671237) and the Natural Science Foundation of Jiangsu Province of China (Grant No. BK20160798).

Reference

Allroggen, F., Malina, R., 2014. Do the regional growth effects of air transport differ among airports? J. Air Transport Manage. 37, 1-4.

Amato, F., Moreno, T., Pandolfi, M., Querol, X., Alastuey, A., Delgado, A., Pedrero, M.,Cots, N., 2010. Concentrations, sources and geochemistry of airborne particulate matter at a major European airport. J. Environ. Monitoring. 12, 854-862.

Anagnostakis, I., Clarke, J.P., Böhme, D., Völckers, U., 2001. Runway operations planning and control: sequencing and scheduling. Journal of Aircraft. 38(6), 988-996.

Ashok, Akshay, Hamsa Balakrishnan, and Steven RH Barrett. 2017. Reducing the air quality and CO2 climate impacts of taxi and takeoff operations at airports. Transportation Research Part D: Transport and Environment, 54, 287-303.

Aviation Environmental Design Tool(AEDT) Technical Manual version 2c, 2016.9:188-191.

Balakrishnan, Hamsa, and Bala Chandran. 2006. Scheduling aircraft landings under constrained position shifting. AIAA Guidance, Navigation, and Control Conference and Exhibit, Keystone, 1~21

Barrett, S.R.H., Yim, S.H.L., Gilmore, C.K., Murray, L.T., 2012. Public health, climate and economic impacts of desulfurizing jet fuel. Environmental Science & Technology. 46, 4275-4285.

Barrett, S.R.H., Britter R. E., Waitz I.A., 2013. Impact of aircraft plume dynamic on airport local air quality, Atmospheric Environment. 74, 247-258.

Barrett, S.R.H., Speth, R.L., Eastham, S.D., Dedoussi, I.C., Ashok, A., Malina, R., Keith, D.W., 2015. Impact of the Volkswagen emissions control defeat device on US public health. Environmental Research Letters. 10, 114005.

Basner, Mathias, et al. Auditory and non-auditory effects of noise on health. The Lancet 383.9925 (2014): 1325-1332.

Baughcum, S.L., Henderson, S.C., Tritz, T.G., 1996. Scheduled civil aircraft emission inventories for 1976 and 1984: Database development and analysis. C1-D11.

Bianco, L., Dell'Olmo, P., Giordani, S., 2006. Scheduling models for air traffic control in terminal areas. Journal of Scheduling. 9(3), 223-253.

Carr, G.C., Erzberger, H., Neuman, F., 1999. Delay exchanges in arrival sequencing and scheduling. Journal of Aircraft. 36(5), 785-791.

Carr, G.C., Erzberger, H., Neuman, F., 2000. Fast-time study of airline-influenced arrival sequencing and scheduling. Journal of Guidance, Control, and Dynamics. 23(3), 526-531.

Carslaw, D.C., Ropkins, K., Laxen, D., Moorcroft, S., Marner, B., Williams, M.L., 2008. Near-field commercial aircraft contribution to nitrogen oxides by engine, aircraft type, and airline by individual plume sampling. Environmental Science& Technology. 42, 1871-1876.

Center E E. User manual for the Base of Aircraft Data (BADA) Revision 3.11. EEC Technical Scientific Report, 2013(14): 22-44.

CCAR, 2016, CCAR 121 Operating requirement: Domestic, flag, and supplemental operations, 657-661.

Chen, J. T., Yousefi, A., Krishna, S., Wesely, D., Sliney, B., Smith, P., 2013. Integrated arrival and departure weather avoidance routing within extended terminal airspace. In: Digital Avionics Systems Conference, 2013 IEEE/AIAA 32nd. IEEE conference proceedings, East Syracuse, New York, USA. pp. 1A4-1.

Clark, C., Stansfeld, S.A., 2011. The Effect of Nocturnal Aircraft Noise on Health: a Review of Recent Evidence. Report prepared for the London Borough of Hounslow, London, UK, p. 36. URL: http://www.hounslow.gov.uk/effect_aircraft_noise_health.pdf.

Deb, K., Pratap, A., Agarwal, S., Meyarivan, T. A. M. T., 2002. A fast and elitist multi objective genetic algorithm: NSGA-II. IEEE transactions on evolutionary computation. 6(2), 182-197.

Dodson, R.E., Houseman, E.A., Morin, B., Levy, J.I., 2009. An analysis of continuous black carbon concentrations in proximity to an airport and major roadways. Atmospheric Environment. 43, 3764-3773.

Dolan, P., Fujiwara, D., 2016. Happiness-Based Policy Analysis. In: Adler, M.D., Fleurbaey, M. (Eds.), The Oxford Handbook of Well-Being and Public Policy. http://www.oxfordhandbooks.com/view/10.1093/oxfordhb/9780199325818.001.0001/oxfordhb-9780199325818-e-9 >.

Dorbian, C. S., Wolfe, P. J., & Waitz, I. A. (2011). Estimating the climate and air quality benefits of aviation fuel and emissions reductions. Atmospheric environment, 45(16), 2750-2759.

Fujiwara, D., Lawton, R.N., MacKerron, G., 2017. Experience sampling in and around airports. Momentary subjective wellbeing, airports, and aviation noise in England. Transportation Research Part D: Transport and Environment. 56, 43–54.

Howarth, D., Griggs, S., 2013. The Politics of Airport Expansion in the United Kingdom: Hegemony, Policy and the Rhetoric of "Sustainable Aviation". Manchester University Press, Manchester, UK.

ICAO, 2008. Doc 9911, Recommended Method for Computing Noise Contours Around Airports.

ICAO, 2014. ICAO Annex 16 Volume II Aircraft Engine Emissions Eighth Edition.

Jin, L., Cao, Y., Sun, D., 2013. Investigation of potential fuel savings due to continuous-descent approach. Journal of Aircraft. 50(3), 807-816.

Kampa, M., Castanas, E., 2008. Human health effects of air pollution. Environmental Pollution. 151, 362-367.

Kim, B., Li, L., Clarke, J.P., 2014. Runway assignments that minimize terminal airspace and airport surface emissions. Journal of Guidance, Control, and Dynamics. 37(3), 789-798.

Kinsey, J.S., Hays, M.D., Dong, Y., Williams, D.C., Logan, R., 2011. Chemical characterization of the fine particle emissions from commercial aircraft engines during the Aircraft Particle Emissions experiment (APEX) 1 to 3. Environmental Science & Technology. 45(8), 3415-3421.

Koudis, G. S., Hu, S. J., Majumdar, A., Jones, R., Stettler, M. E. (2017). Airport emissions reductions from reduced thrust takeoff operations. Transportation Research Part D: Transport and Environment, 52, 15-28.

Kurniawan, J.S., Khardi, S., 2011. Comparison of methodologies estimating emissions of aircraft pollutants, environmental impact assessment around airports. Environmental Impact Assessment Review. 31, 240-252.

Marais, Karen B., et al. 2013, Evaluation of potential near-term operational changes to mitigate environmental impacts of aviation. Proceedings of the Institution of Mechanical Engineers, Part G: Journal of Aerospace Engineering. 227(8), 1277-1299.

Masiol, M., Harrison, R.M., 2014. Aircraft engine exhaust emissions and other airport-related contributions to ambient air pollution: A review, Atmospheric Environment. 95, 409-455.

Mitchell, D., Ekstrand, H., Prats, X., Grönstedt, T., 2012. An environmental assessment of air traffic speed constraints in the departure phase of flight: A case study at Gothenburg Landvetter Airport, Sweden. Transportation Research Part D: Transport and Environment. 17, 610-618.

National Standard of People's Republic of China, Measurement of aircraft noise around airport, GB9661-88,1988,4-5.

Penn, S.L., Boone, S.T., Harvey, B.G., 2017. Modeling variability in air pollution-related health damages from individual airport emissions. Environmental Research. 156, 791-800.

Pfeil, D.M., 2011. Optimisation of airport terminal-area air traffic operations under uncertain weather conditions. Ph.D. MIT.

Pfeil, D.M., Balakrishnan, H., 2012. Identification of robust terminal-area routes in convective weather. Transportation Science. 46(1), 56-73.

Płanda, Beata, and Jacek Skorupski, 2017. Methods of air traffic management in the airport area including the environmental factor. International Journal of Sustainable Transportation. 11(4), 295-307.

Prete, J., Mitchell, J.S., 2004. Safe routing of multiple aircraft flows in the presence of time-varying weather data. In: Guidance, Navigation, and Control Conference (GNC), 2004 AIAA. AIAA conference proceedings, Providence, Rhode Island. AIAA, 2004-4791.

Rodríguez Díaz, A., Díaz Fernández, B. A., González Torre, P.L., 2017. A review of the impact of noise restrictions at airports. Transportation Research Part D: Transport and Environment. 50, 144–153.

Sidiropoulos, S., Han, K., Majumdar, A., & Ochieng, W.Y., 2017. Robust identification of air traffic flow patterns in Metroplex terminal areas under demand uncertainty. Transportation Research Part C: Emerging Technologies. 75, 212-227.

Silva, B., Eller, R., Santos, E., 2013. Environment Improvements with RNP Procedures the Santos Dumont Airport Case. In: World Conference on Transport Research, 2013 13th. Elsevier, Rio de Janeiro, Brazil. pp. 1-13.

Simaiakis, I., Khadilkar, H., Balakrishnan, H., Reynolds, T. G., Hansman, R. J., 2014. Demonstration of reduced airport congestion through pushback rate control. Transportation Research Part A: Policy & Practice. 66(1), 251-267.

Sölveling, Gustaf., Solak, S., Clarke, J.P.B, Johnson, E.L., 2011. Scheduling of runway operations for reduced environmental impact. Transportation Research Part D: Transport and Environment. 16, 110-120.

Srinivas, N., Deb, K., 1994. Multi objective optimization using nondominated sorting in genetic algorithms. Evolutionary computation. 2(3), 221-248.

Torija, Antonio J., and Rod H. Self., 2018. Aircraft classification for efficient modelling of environmental noise impact of aviation." Journal of Air Transport Management 67, 157-168.

Wan, L., Hu, M., Tian, Y., Zhang, S., 2016. Optimizaiton model of arrival and departure resource allocation in terminal area. Journal of Traffic Transportation Engineering. 16(2), 109-117.

Wolfe, P. J., Malina, R., Barrett, S. R., & Waitz, I. A. (2016). Costs and benefits of US aviation noise land-use policies. Transportation Research Part D: Transport and Environment, 44, 147-156.

Yin, J., Hu, M., and Peng, Y., 2014a. Optimized method for multi-runway spatio-temporal resource scheduling in mode of dependent approaches. Acta Aeronautica et Astronautica Sinica. 35(11), 3064-3073.

Yin, J., Hu, M., and Zhang, H., 2014b. Optimization approach for collaborative operating modes of multi-runway systems. Acta Aeronautica et Astronautica Sinica. 35(3), 795-806.

Zhang, Z., Wang C., Meng N., Gao, C., 2014. A Noise Evaluation of Flight Procedures Method Based on Trajectory Segmentation. Science Technology and Engineering. 14(3), 116-120.